Argonne NATIONAL LABORATORY

ANL/NSE-22/59

Modeling of a Generic Pebble Bed High-temperature Gas-cooled Reactor (PB-HTGR) with SAM

Nuclear Science and Engineering Division

ANL/NSE-22/59

Modeling of a Generic Pebble Bed High-temperature Gas-cooled Reactor (PB-HTGR) with SAM

prepared by
Zhiee Jhia Ooi, Ling Zou, Thanh Hua, Jun Fang, Rui Hu
Nuclear Science and Engineering Division, Argonne National Laboratory

September 2022

ABSTRACT

This report presents the modeling of the core of a generic pebble-bed reactor (PBR) at the system level using the System Analysis Module (SAM) code. This work is an extension of a previous work by the authors (Ooi et al. (2021)) that used the so-called 2-D ring model approach to model the PBMR-400. With the new approach, the pebble bed of the reactor is modeled with multiple *PBCoreChannel* components with spherical heat structures which allows the code to calculate thermal fluid parameters with built-in closure relations. The new core-channel approach is an improvement to the 2-D ring model approach as it does not introduce geometric distortions to the model and thus reduces the uncertainties of the predictions. In addition to thermal fluid simulations, point kinetics (PKE) are included to the model. Simulations are performed under a steady-state normal operation condition and a load-following transient scenario. This particular transient scenario is chosen as it tests both the thermal fluid and neutronics aspects of the model. The predicted results from both the steady-state and transient scenarios are compared with the results by Stewart et al. (2021) who performed similar simulations with a Griffin-Pronghorn coupled tool. Despite the differences between the codes, with SAM being a system-analysis code and Pronghorn being a porous-medium code, both sets of results compare favorably. The overall profiles and trends of the predicted temperatures and reactivities from the SAM and Griffin/Pronghorn simulations are similar, with some differences in their predicted values. The first part of the report covers the significance of a relatively fast-running approach that is capable of modeling the pebble bed reactor at the system-level while simultaneously capturing the radial thermal behavior of the core. Then, the modeling approach used in this work is discussed in details. Lastly, the results and comparisons with the Griffin/Pronghorn simulation are presented.

Keywords: High-temperature gas-cooled reactor, pebble bed reactor, system-level modeling, load-following transient, SAM

Contents

List of Figures

List of Tables

1 Introduction

The high-temperature gas-cooled reactor (HTGR) is one of the candidates for the Gen-IV reactor designs that is currently being developed worldwide. Among the HTGRs, the pebble bed reactor (PBR) has attracted a lot of interests due to its design features such as low excess reactivity and online refueling (Balestra et al. (2021)). Given the increasing reliance on computational tools for the determination of safety margin and regulatory justification in the development of new reactor designs, it is important that these tools are properly tested and verified.

Compared with the conventional light water reactors, the pebble bed reactors have complex core geometries that result in more complicated thermal-fluid behaviors in the reactor core during both steady-state normal operating condition and transient scenarios. Furthermore, the reliance on reactor cavity cooling system (RCCS) by these reactors for decay heat removal during certain transients introduces further challenges that need to be resolved in the modeling of these reactors. In the conventional light water reactors, heat is removed primarily through convective heat transfer between the fuel rods and the coolant during both steady-state operating condition and transient scenarios. The only differences are the source of the coolant (e.g., driven by coolant pumps compared with injection by emergency core cooling systems (ECCS)) and the switch from single-phase convective heat transfer to two-phase boiling heat transfer. On the other hand, for PBRs and other HTGR designs in general, the heat removal mechanisms during steady-state operating condition and transient scenarios could be substantially different.

Under steady-state operating condition, similar to light water reactors, heat is removed mainly by forced convection between fuel pebbles and the coolant, with the coolant being some type of gas rather than water. However, during loss-of-forced flow transient scenarios, unlike light water reactors, decay heat is primarily removed from the core via radial heat conduction from the pebble fuels to the side reflectors and finally to the RCCS. In the former, heat transfer is a localized phenomenon with a relatively small length scale in the order of several centimeters. Conversely, during loss-of-forced flow transient scenarios, the core-wise radial conduction from the pebble bed to the RCCS adds another heat transfer length scale that corresponds to the the reactor core diameter in the order of several meters. Furthermore, natural convection can establish in the core during the loss-of-forced flow transients which can further impact the temperature redistribution inside the reactor core and thus the removal of decay heat. The combination of different heat removal mechanisms poses a unique set of challenges to the modeling of the PBRs.

Various modeling approaches have been used to model the PBRs at various length and time scales. For example, the unit-cell approach is used by van Antwerpen et al. (2012) to calculate the effective thermal conductivity in packed pebble beds. In this approach, pebbles are usually packed into a unit cell where the local thermal fluid interaction between the pebbles and the coolant as well as between adjacent pebbles are studied. While the unit cell approach is generally less complex and less computationally expensive than other high-fidelity simulations, the main challenge of this approach is finding a representative unit cell that can capture the the correct thermal fluid behaviors of pebbles and coolant in an actual reactor. On the other hand, high-fidelity CFD simulations are employed by researchers to study the heat transfer and fluid flow surrounding fuel pebbles. Depending

on the objectives of these studies, the simulations employ lower-resolution approaches such as the Reynolds-averaged Navier-Stokes methods (RANS) to high resolution approaches such as Large Eddy Simulation (LES) and Direct Numerical Simulation (DNS) methods. Similarly, the simulation domain can range from a single fuel pebble to multiple pebbles or even a full core of pebbles. As shown by Merzari et al. (2021), full-core simulation of the pebble bed fluoride-salt-cooled high-temperature reactor (PB-FHR) with LES has been achieved using Cardinal, which is a lower-length-scale simulator that comprises three physics: neutronics, thermal fluids, and fuel performance.

Despite the advancement of computational technology, such high-fidelity simulations can be prohibitively expensive, particularly for the simulations of transient scenarios that can span several days. Thus, there exists a need for a modeling approach that can capture the core-wide behavior of a reactor, while at the same time, can remain relatively fast-running compared to CFD simulations. Such an approach, known as the system-level simulation, intends to capture the most important phenomena of reactor transients, sometimes known as the "figure of merits," such as peak fuel temperature, in an averaged sense. Due to the lower details and resolutions, system-level simulation tends to be less computationally expensive and thus fast-running, making it an ideal analysis tool to simulate long transient scenarios. In recent studies, Pronghorn (Novak et al. (2021)), a multiscale thermal-hydraulic code, is used to model the PBMR-400 (Balestra et al. (2021)) and the generic 200 MW pebble bed reactor (Stewart et al. (2021)), where the fuel pebble bed in the core is treated as a porous medium. On the other hand, in a previous work by the authors of this work (Ooi et al. (2021)), the PBMR-400 is modeled with the System Analysis Module (SAM) code (Hu et al. (2021)) using the so-called 2-D ring model approach. With this approach, the pebble fuels are arranged into layers of cylindrical rings separated by coolant channels. Geometric corrections are then applied to the alternating layers of fuel and channel rings to ensure that the thermal fluid behaviors are modeled correctly. The 2-D ring model captures the core-wide behavior while at the same time remains sufficiently fast-running for long transients.

This work aims to develop an improved approach to model the core of the generic PBR at the system level with SAM. In this approach, the core is modeled with the *PBCoreChannel* component in spherical geometry. Unlike the 2-D ring model approach, the core channel approach does not involve geometric modification such that the uncertainties introduced to the model due to geometry correction is avoided, and therefore the accuracy of the simulation is improved. In this study, two types of conditions of the generic PBR is considered: a steady-state normal operating and a load-following transient condition. For the remainder of this report, the overall layout of the core and the modeling approach is discussed in details, followed by discussions on the results from the steady-state and transient simulations.

2 Model Description

2.1 Core geometry

The 200 MW(thermal) generic pebble bed reactor is chosen as the reference design in this work, focusing only on the core. Auxillary components that make up the coolant

system of the reactor are not included here to reduce the complexity of the model so that the thermal hydraulics and neutronics behavior of the core could be properly studied. The design information of the reactor used here is obtained from the work by Stewart et al. (2021) based on publicly available figures and models. The reactor has an installed thermal capacity of 200 MW, cooled by pressurized helium gas with the primary coolant pressure of 6 MPa, inlet and outlet core temperatures of 533 K and 1023 K, respectively, and a nominal helium mass flow rate of 78.6 kg/s during steady-state normal operating condition. The pebble bed core has a packing factor of 0.61 and roughly 223,000 pebbles are loaded. The schematic of the generic PBR core is shown in Figure 2.1 and the dimensions of the core are tabulated in Table 2.1.

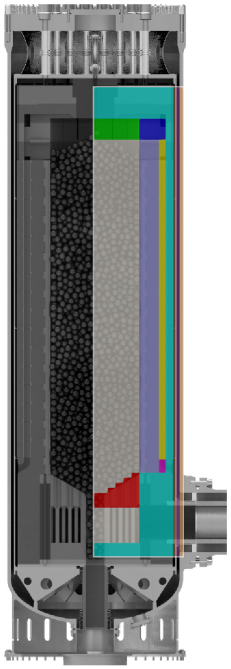

Figure 2.1: Schematic of the core of the generic pebble bed reactor (Stewart et al. (2021)).

2.2 General descriptions

Based on the schematic shown in Figure 2.1 and the dimensions tabulated in Table 2.1, a SAM model for the generic PBR core is built. The schematic of the SAM model is shown in Figure 2.2 with the assumption that the core is axially symmetric. In the SAM model, solid structures such as the reflectors, core barrel, reactor pressure vessel, and RCCS panels are modeled with the *PBCoupledHeatStructure* components. Meanwhile, coolant channels such as the upcomer and flow channels in the bottom reflector are modeled as one-dimensional flow with the *PBOneDFluidComponent*.

The pebble bed is modeled with multiple *PBCoreChannel* components, each of which effectively represents a column of cylindrical or annulus of pebble bed. Note that the *PBCoreChannel* is essentially a one-dimensional fluid component with built-in heat structures

Table 2.1: Dimensions of the generic PBR core (Stewart et al. (2021)).

Features	Dimensions [m]
Core radius	1.20
Reflector width between core and riser	0.52
Riser width	0.18
Outer reflector width	0.21
Gap between reflector and barrel	0.04
Barrel thickness	0.04
Gap between barrel and reactor pressure vessel	0.08
Reactor pressure vessel thickness	0.09
Bottom reflector height	0.54
Core height	8.91
Core inlet height	0.36
Riser height	8.57
Top gap height	0.55
Top reflector height	0.85

that can simulate solid-to-fluid thermal fluid behaviors. This allows the specification of hydraulic parameters such as flow area, hydraulic diameter, and surface roughness, as well as solid parameters such as the geometry and material properties of the heat structure. Additionally, heat transfer parameters such as the heat transfer area density can be provided to the component. Solid, fluid, and heat transfer behaviors are then calculated internally by the *PBCoreChannel* component according to the provided information. In this model, the *PBCoreChannel* component is set to have spherical heat structures where the heat-transfer geometry is set as pebble bed. The use of multiple *PbCoreChannels* in the radial direction allows the model to capture the radial heat conduction within the pebble bed and from the pebble bed core to the reflectors, which is particularly important for loss-of-forced flow transient scenarios where radial conduction plays a significant role in decay heat removal. Furthermore, the angled fuel chute at the bottom of the pebble bed is modeled with multiple smaller *PBCoreChannels* to roughly capture the geometry of that region. The total power of the core during steady-state operation is set to 200 MW. Axial and radial power shape functions obtained from the work by Stewart et al. (2021) are prescribed to the core to ensure the correct temperature distribution in the core.

The bottom reflector located below the pebble bed core is a porous region that allows the coolant to flow through. In the SAM model, this region is modeled as alternating layers of *PBCoupledHeatStructure* and *PBOneDFluidComponent*. The width of the heat structures and channels are determined based on the porosity of this region of 0.25.

2.3 Thermal coupling of components

To correctly model the heat transfer between components, adjacent components are thermally coupled to each other. The coupling between *PBCoupledHeatStructures* and *PBOneDFluidComponents* are done readily with the *name_comp_left* and *name_comp_right* options in *PBCoupledHeatStructures*. For *PBCoreChannels*, the heat transfer surface area,

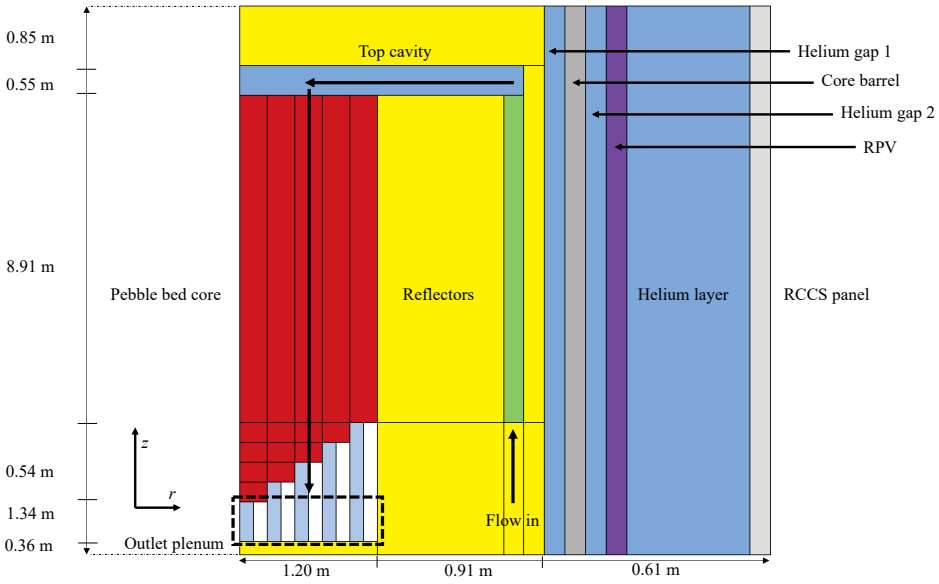

Figure 2.2: Schematic of the SAM PBR core model (not to scale).

a_w between the solid and fluid structures can be set using the *HT_surface_area_density* option. For each core channel, a_w is defined as the ratio of the total surface area of heat structures in the core channel to the total fluid volume as,

$$a_w = \frac{4\pi r_{pebble}^2 n_{pebble}}{V_{core}\varepsilon}, \tag{2.1}$$

where r_{pebble}, n_{pebble}, V_{core}, and ε are the radius of fuel pebble, number of fuel pebbles in the core channel, the total volume of core channel, and the pebble bed porosity that is equal to 1 - packing factor, respectively. The correct a_w is important to ensure the correct energy balance between the solid and fluid components. The heat transfer coefficient in the *PbCoreChannels* is calculated using SAM's built-in KTA correlation, as suggested by the PBMR-400 transient benchmark report by the Nuclear Energy Agency (NEA (2013)),

$$\mathrm{Nu} = 1.27\frac{\mathrm{Pr}^{1/3}}{\varepsilon^{1.18}}\mathrm{Re}^{0.36} + 0.033\frac{\mathrm{Pr}^{1/2}}{\varepsilon^{1.07}}\mathrm{Re}^{0.86} \tag{2.2}$$

where Pr and Re are the Prandtl and Reynolds numbers.

To model the radial heat conduction in the pebble bed, the heat structures of adjacent *PBCoreChannels* need to be thermally coupled to each other. This is done using SAM's *SurfaceCoupling* component of type *PebbleBedHeatTransfer*. The *SurfaceCoupling* component requires the specification of *h_gap* which dictates the heat transfer capability between two coupled components. For the *PBCoreChannels*, *h_gap* is determined using the ZBS correlation (Zou and Hu (2019); van Antwerpen et al. (2010)) which calculates the effective thermal conductivity of the pebble bed core with the consideration of pebble-pebble conduction, pebble-coolant convection/conduction, pebble-pebble radiation,

$$\frac{k_{eff}}{k_f} = \left(1-\sqrt{1-\varepsilon}\right)\varepsilon\left[\left(\varepsilon-1+\frac{1}{\kappa_G}\right)^{-1}+\kappa_r\right]+\sqrt{1-\varepsilon}\left[\varphi\kappa+\left(1-\varphi\right)\kappa_c\right]. \tag{2.3}$$

where φ is the surface fraction parameter for heat transfer through contact areas. The non-dimensional effective thermal condcutivity related to fluid phase conduction, κ_G is simplified to be 1. For the non-dimensional effective thermal conductivity related to thermal radiation, κ_r, and the contribution from the heat transfer due to solid conduction, fluid conduction, and thermal radiation, κ_c, more detailed descriptions are available in the aforementioned references.

Note that the ZBS correlation provides the effective thermal conductivity of the pebble bed core but not the heat transfer coefficient, which is the parameter needed for the *SurfaceCoupling* component. To obtain the heat transfer coefficient, the effective thermal conductivity from the ZBS correlation is divided by a characteristic length-scale, ΔL, as,

$$h_{gap} = \frac{k_{ZBS}}{\Delta L}. \tag{2.4}$$

In this work, the characteristic length-scale is chosen to be the distance between the centers of adjacent *PbCoreChannels*.

Similar approach is used to couple the outermost *PBCoreChannel* to the inner wall of the side reflector to allow heat from the core channel to escape to the reflector and eventually to the RCCS. The *h_gap* is calculated using the correlation by Hahn and Achenbach (1986),

$$\mathrm{Nu}_w = \left(1-\frac{1}{D_w/L_f}\right)\mathrm{Re}^{0.61}\mathrm{Pr}^{1/3}, \tag{2.5}$$

where D_w and L_f are the inner diameter of the reflector and the characteristic length scale (pebble diameter), respectively.

Furthermore, as shown in Figure 2.1, due to geometric restriction, the reflector in the SAM model consists of multiple individual sections. The surfaces of adjacent reflector sections are thermally coupled in the axial and radial directions using a similar approach as described previously with the only difference being that the *SurfaceCoupling* component is set to type *GapHeatTransfer*. The *h_gap* is set to an arbitrarily large value of 1×10^8 W/m^2 to ensure temperature continuity across different sections. Lastly, the heat transfer across helium layers between different surfaces near the outer edge of the core is modeled with radiative heat transfer. This is once again done using the *SurfaceCoupling* with type *RadiationHeatTransfer* where the surface emissivity of all components are set as 0.8 as suggested by the NEA (2013) report.

2.4 Point kinetics

Point kinetics are included in the model for the transient load-following simulation. The point kinetics parameters such as the delayed neutron fractions, the neutron lifetimes, the delayed neutron precursor decay constant, the prompt neutron lifetime, and the reactivity feedback coefficients are obtained from the work by Stewart et al. (2021), in which these parameters were generated with the nuetronics code Griffin. The prompt neutron generation

time, Λ is 6.519×10^{-4} s while the delayed neutron fraction, β_i, and the delay neutron precursor decay constant, λ_i are tabulated in Table 2.2.

Table 2.2: PKE parameters from Griffin by Stewart et al. (2021).

Groups	β_i [-]	λ_i [1/s]
1	2.344×10^{-4}	1.334×10^{-2}
2	1.210×10^{-3}	3.273×10^{-2}
3	1.150×10^{-3}	1.208×10^{-1}
4	2.588×10^{-3}	3.029×10^{-1}
5	1.070×10^{-3}	8.501×10^{-1}
6	4.486×10^{-4}	2.855

In this model only temperature reactivity feedback from the fuel, moderator, and reflector regions are considered. Other mechanisms such as coolant reactivity feedback, xenon reactivity feedback, and core expansion reactivity feedback were not considered in the work by Stewart et al. (2021), and therefore not included in this work for a fair code-to-code comparison purpose. The distribution of local reactivity coefficients are illustrated in Figure 2.3 where the reactivity of the pebble bed is shown to be influenced by the feedback from the fuel, moderator, and reflector. To properly account for the reactivity feedback from different regions, it is necessary to divide the pebble heat structures into three layers of fuel, moderator, and reflector with the correct reactivity coefficients prescribed to each layer. Furthermore, this step is necessary because SAM treats fuel (Doppler) reactivity coefficients differently than moderator/reflector reactivity coefficients. Note that no such distinction is made by SAM between the moderator and reflector reactivity coefficients. This means that in the reflector region where the fuel (Doppler) reactivity coefficients are absent, the local moderator and reflector reactivity coefficients from Griffin are summed and prescribed directly to the heat structures.

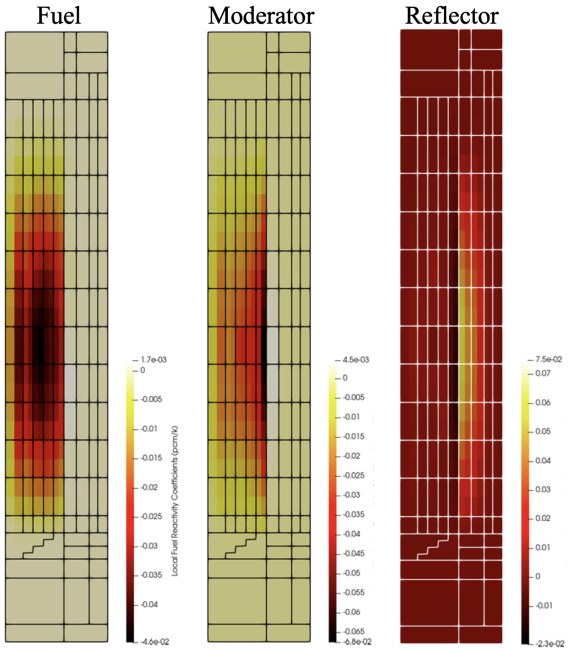

Figure 2.3: Distributions of reactivity feedback coefficients of fuels, moderators, and reflectors from Griffin by Stewart et al. (2021).

3 Simulation Results

3.1 Steady-state

A steady-state normal operation case is set up to verify the SAM model. The steady-state condition has an inlet helium mass flow rate of 78.6 kg/s and an inlet temperature of 533 K and a constant-pressure outlet boundary condition of 6 MPa. The outer surface of the RCCS panels is set to a constant temperature of 293.15 K. The reactor has a steady-state power of 200 MW.

Figure 3.1 shows a qualitative comparison of the reflector temperature distribution between the SAM and Griffin/Pronghorn simulations by Stewart et al. (2021). Note that the temperature distribution in the pebble bed core is not shown here and will be discussed later because the heat structures in each of SAM's *PBCoreChannel* appear as a one-dimensional line. Overall, a good agreement is observed between SAM's and Griffin/Pronghorn's results where the temperature distributions appear to be similar with the upper half of the core being at a lower temperature compared to the bottom half. The bottom reflectors located under the pebble bed core appear to be the hottest, with a peak temperature of roughly 1100 K in both cases. Furthermore, most of the outer reflectors appear to be in a relatively low temperature compared to the bottom reflectors. This indicates that during steady-state normal operation, only a small amount of heat is conducted radially from the core to the outer reflectors as forced convection is the primary heat removal mechanism in the core.

The radial distributions of the maximum, minimum, and mean fuel and kernel temperatures in the pebble bed from SAM are shown in Figure 3.2. Note that 'fuel' denotes the

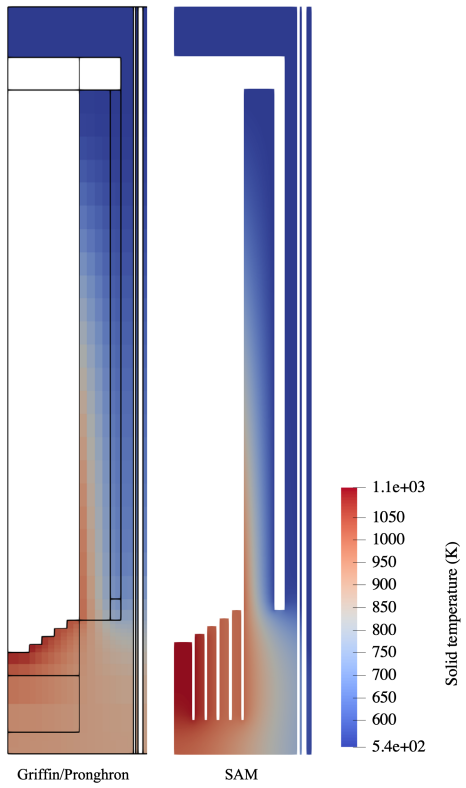

Figure 3.1: Qualitative comparison of the steady-state reflector temperature between the SAM and Pronghorn simulations (Stewart et al. (2021)).

overall matrix temperature of the pebbles. The temperature decreases from the innermost to the outermost core channels, following the radial distribution of the power prescribed to the core channels. Additionally, the close proximity of the outer channels to the reflectors allows heat from these channels to escape to the reflectors, further lowering their temperatures. As expected, the kernel temperature is consistently higher than the fuel/matrix temperature.

The solid and fluid axial temperature profiles in the pebble bed core from SAM and Griffin/Pronghorn are compared in Figure 3.3 and Figure 3.4, respectively. Note that SAM's results are represented by the solid lines while Griffin/Pronghorn's results are represented by the dashed lines. The overall trends between the two sets of simulations are largely similar. For the solid temperature, a good agreement is observed between SAM and Griffin/Pronghorn in the upper half of the core. However, in the bottom half, SAM predicts a slightly higher solid temperature in the two innermost core channels, namely 'F-1' and 'F-2'. Both models predict a small increase of temperature in the fuel chute, likely due to reduced heat transfer from the fuel pebbles to the surrounding reflectors. The fluid temperature profiles from SAM and Griffin/Pronghorn show good agreement where they have similar trend as the solid temperatures. In general, the SAM-predicted temperatures in these channels show a wider spread as the pebble bed is modeled as *PBCoreChannels*

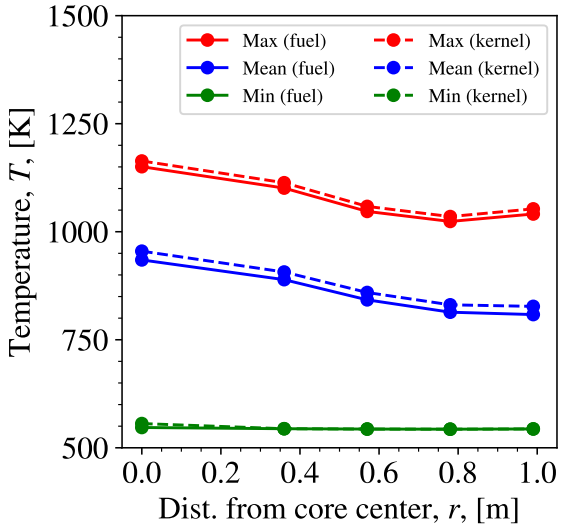

Figure 3.2: Radial distributions of fuel and kernel temperatures in the pebble bed from SAM.

where thermal coupling is possible, but flow mixing is not captured. On the contrary, Pronghorn uses porous medium flow to model the core, such that the helium temperature is relatively more uniform. Lastly, SAM predicts an average coolant outlet temperature of 1020 K, which is 4 K lower than Griffin/Pronghorn's prediction of 1024 K (Stewart et al. (2021)).

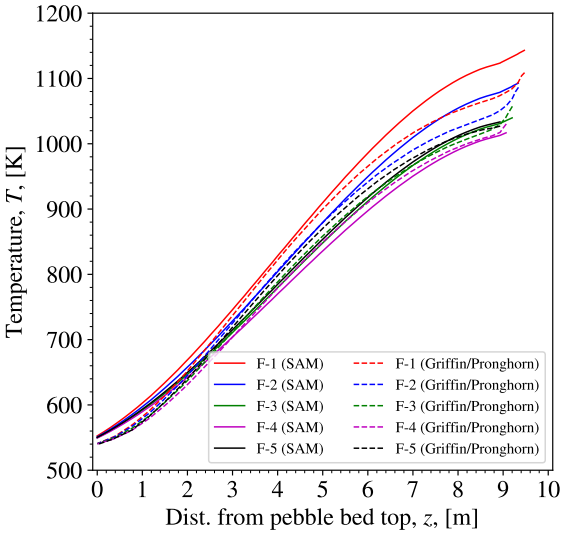

Figure 3.3: Comparison of the steady-state solid temperature axial profiles between SAM and Griffin/Pronghorn (Stewart et al. (2021)).

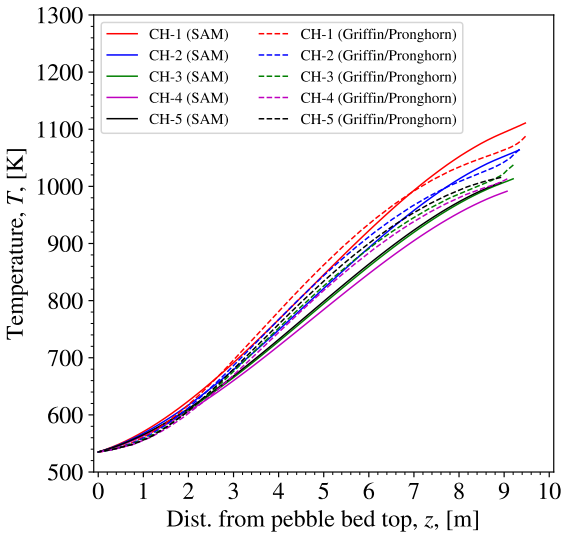

Figure 3.4: Comparison of the steady-state coolant temperature axial profiles between SAM and Griffin/Pronghorn (Stewart et al. (2021)).

3.2 Load-following transient

For the transient analysis, a load-following case with a varying inlet mass flow rate is selected, similar to the 100-40-100 load following exercise of PBMR-400 suggested by the NEA (2013) report. This case is chosen for this work because it tests not only the thermal hydraulics modeling of SAM but also its neutronics modeling with the point kinetics equations (PKE). The six-group formulation of the PKE is used here with parameters such as the delayed neutron fraction, precursor decay constant (tabulated in Table 2.2), and the local reactivity coefficients obtained from the Griffin/Pronghorn simulation (Stewart et al. (2021)).

Temperature reactivity feedbacks are modeled in the pebble bed core and the surrounding reflectors. Note that coolant density and fuel axial expansion feedbacks are not included here. The reactivity coefficients are divided into three groups, namely the coefficients for the fuel, moderator, and reflector regions whose distributions are shown in Figure 2.3. The fuel and moderator coefficients contribute primarily to the reactivity feedback in the pebble bed core with a small amount of contribution from the reflector coefficients near the outer edge of the pebble bed core. Meanwhile, the reflector coefficients are responsible for the reactivity feedback in the reflector regions. The reactivity feedback of the fuels is determined based on the fuel kernel temperature, which in SAM is calculated using the model by TINTE (Gerwin et al. (2010)) while the reactivity feedbacks for the reflectors and moderators are calculated with the solid temperature. Given the difference in the temperature used for calculating the reactivity feedback in the pebble bed core, the heat structures in the pebble bed core are divided into three layers of fuel, moderator, and reflector where each layer is prescribed with a reactivity coefficient according to its type. Such distinction is not necessary in the reflector region surrounding the pebble bed core because the reactivity feedback in this region depends almost entirely on the reflector coefficients.

As shown in Figure 3.5, the inlet flow rate is reduced from the nominal value of 78.6 kg/s (100%) to 19.65 kg/s (25%) over the course of 15 minutes. The flow rate is kept at 25% for 30 minutes before it is ramped back up to 100% over 15 minutes.

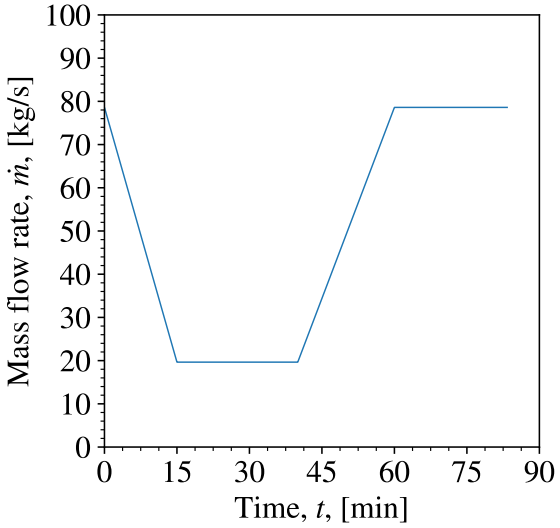

Figure 3.5: Coolant mass flow rate for the load-following transient simulation.

The reactivities and reactor power predicted by SAM and Griffin/Pronghorn (Stewart et al. (2021)) during transient are shown in Figure 3.6 and Figure 3.7, respectively. Note that the SAM results are represented by the solid lines while the Griffin/Pronghorn results are the dashed lines. Despite some differences in both sets of predictions, their overall trends agree relatively well. When flow rate is decreased, the reduction in heat removal from the fuel causes the overall core temperature to rise, leading to negative total reactivity, which in turn decreases the reactor power. As the flow rate is held constant at 25%, the change of temperature decreases and causes the reactivity to be near zero. Conversely, when the flow rate is increased, the overall core temperature decreases suddenly due to improved heat removal. The reactivity shows a sharp increase and becomes positive, raising the reactor power, before gradually decreasing back to zero as the temperature stabilizes.

During transient, the power decreases linearly from the nominal value of 200 MW to roughly 55 MW as flow rate is decreased. The power maintains at this level for the next 30 minutes as the flow rate is held constant before rising back to the nominal value as the flow rate is ramped back up. The power predicted by SAM is consistently lower than Griffin/Pronghorn's prediction by approximately 2 MW, which is likely caused by the difference in the reactivities predicted by both simulations.

The mean fuel and kernel temperatures, moderator temperature, and reflector temperature predicted by SAM are shown in Figure 3.8, Figure 3.9, and Figure 3.10, respectively. Note that the SAM results shown here are the volume-averaged temperature of a particular component. Volume-averaging is necessary to ensure that the mean temperatures are not skewed by the number of sections of a component. For instance, due to its complex geometry, the lower reflector region is comprised of a greater number of sections compared to the

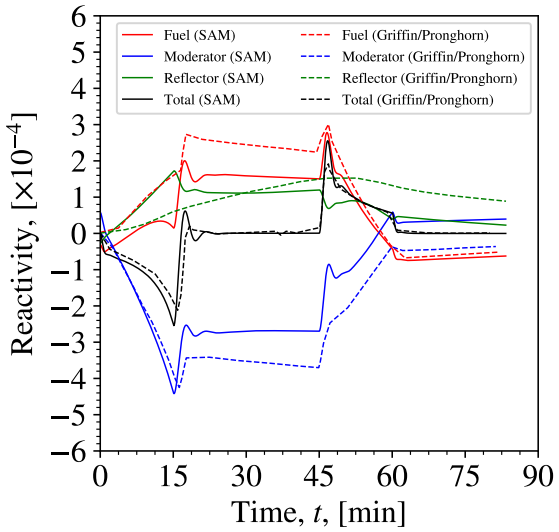

Figure 3.6: Reactivities predicted by SAM in the load-following transient simulation.

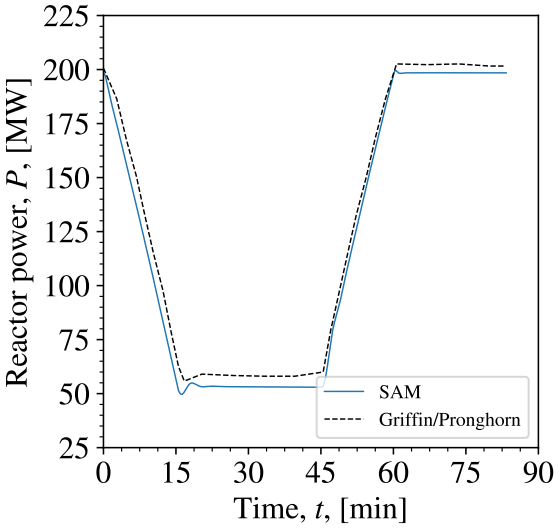

Figure 3.7: Total reactor power predicted by SAM in the load-following transient simulation.

side reflector which has a comparatively simpler geometry. Thus, without volume-averaging, the mean temperature will be skewed towards the lower reflector region.

For the SAM prediction, during the initial ramp down, despite the increasing fuel temperature, the kernel temperature decreases due to the reduction of reactor power as shown in Figure 3.7. As the fuel (Doppler) reactivity feedback is calculated with the kernel temperature, a decrease in the kernel temperature causes the fuel reactivity to increase. At the same time, the moderator temperature increases and leads to a decrease of reactivity. On the other hand, given that the reflector reactivity coefficients are primarily positive, an increase in the reflector temperature causes the reflector reactivity to increase. It is also

observed that the total reactivity is dominated by the moderator reactivity. During the constant flow rate stage, the kernel, moderator, and reflector temperatures are relatively unchanged with each experiencing minor changes. As a result, the respective reactivities remain largely constant and produce a total reactivity of approximately zero.

Lastly, during the ramp up stage, the fuel and kernel temperatures increase and cause the reactivity of the fuel to decrease. Conversely, the increased coolant flow reduces the moderator temperature and leads to an increase of moderator reactivity. The reflector temperature also decreases in this stage, resulting in a decrease of reflector reactivity. The resultant total reactivity shows a sharp initial increase before dropping gradually as the flow rate is increased back to the nominal level.

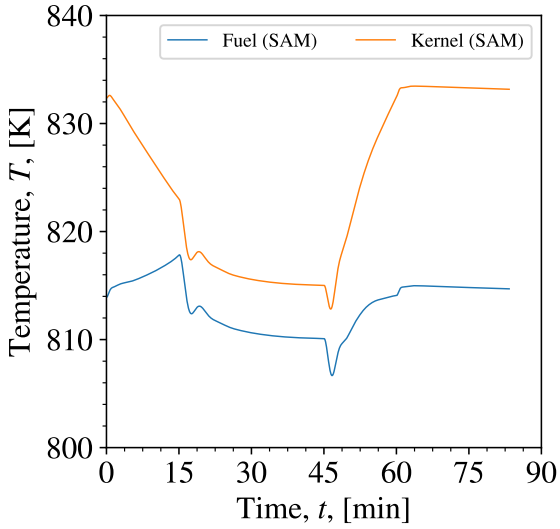

Figure 3.8: Average fuel and kernel temperatures predicted by SAM in the load-following transient simulation.

As discussed in Section 3.1, given that the SAM and Griffin/Pronghorn models are essentially two different approaches, some differences inevitably exist between the steady-state temperatures predicted by both models. Furthermore, these differences could be further exaggerated during transient. Hence, a direct comparison of temperatures between the two sets of results could be misleading. As a result, it is more insightful to compare the evolution of temperature of different regions in the reactor during transient. To achieve that, the temperature changes, ΔT, of the fuel, moderator, and reflector are shown in Figure 3.11, Figure 3.12, and Figure 3.13, respectively. Note that ΔT is defined as the difference between the temperature at the start of transient and the temperature during transient,

$$\Delta T = T(t = 0) - T(t = t'), \tag{3.1}$$

where t' is the time during transient. It should be pointed out that a positive ΔT represents a drop in temperature while a negative ΔT represents an increase in temperature with respect to the temperature at the start of transient.

As shown in Figure 3.11, the change in fuel temperature predicted by Griffin/Pronghorn

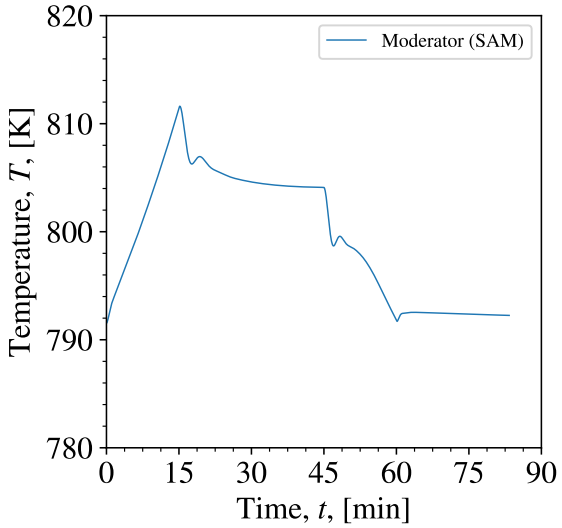

Figure 3.9: Average moderator temperature predicted by SAM in the load-following transient simulation.

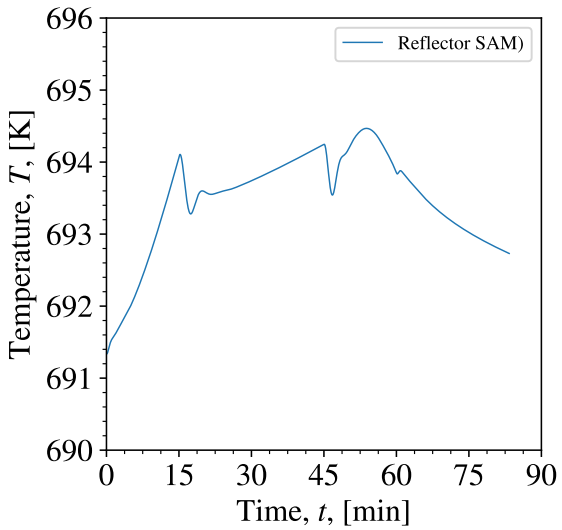

Figure 3.10: Average reflector temperature predicted by SAM in the load-following transient simulation.

and SAM are relatively similar during the flow ramp down phase, with the prediction from SAM showing a larger increase of temperature due to a reduction in heat removal by the coolant. However, during the constant-flow phase, the SAM prediction shows a decrease of temperature ranging from 1-4 K while the Griffin/Pronghorn prediction is relatively uniform with only a small increase of temperature of roughly 1-2 K. The difference in trends could be attributed to the difference in power generated by the core where the SAM prediction experiences a drop of roughly 500 kW of core power over the same period, thus leading to a

small decrease in fuel temperature. Finally, in the ramp up phase, the differences from both models start to converge and eventually arrive at a reasonably good agreement once the mass flow rate is returned to the nominal level. It should also be pointed out that similar 'spikes' are observed in both sets of results at the termination of flow ramp down (15 min) and the initiation of flow ramp up (45 min).

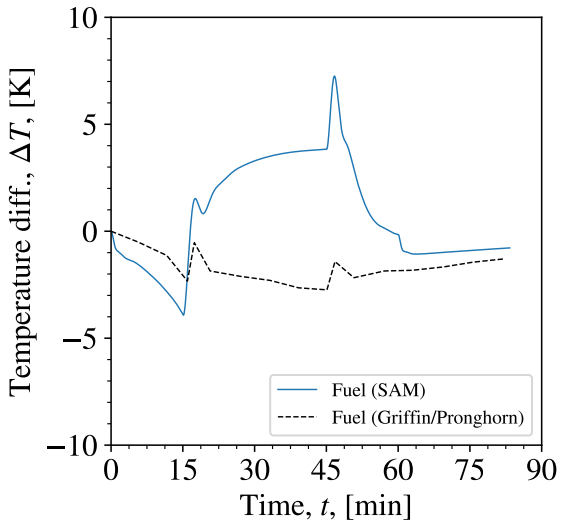

Figure 3.11: Comparison of the fuel temperature change predicted by SAM and Griffin/Pronghorn.

The comparison of the change in moderator temperature is shown in Figure 3.12 where the predictions from both models are observed to have a good overall agreement. In the flow ramp down phase, the increase of moderator temperature predicted by SAM and Griffin/Pronghorn are almost the same with that by SAM being consistently greater by roughly 1 K. In the constant-flow phase, the temperature change predicted by SAM and Griffin/Pronghorn start to diverge as the reactor power predicted by SAM experiences a small decrease. However, the difference diminishes when the flow is ramped up to its nominal value, which is similar to the behavior of the fuel temperature discussed previously. Finally, the change of reflector temperature is shown in Figure 3.13. It is seen that the predictions from both models agree well with each other in terms of the overall trend and magnitude, with the only difference being the prediction by Griffin/Pronghorn showing a smoother change over time compared to SAM's prediction.

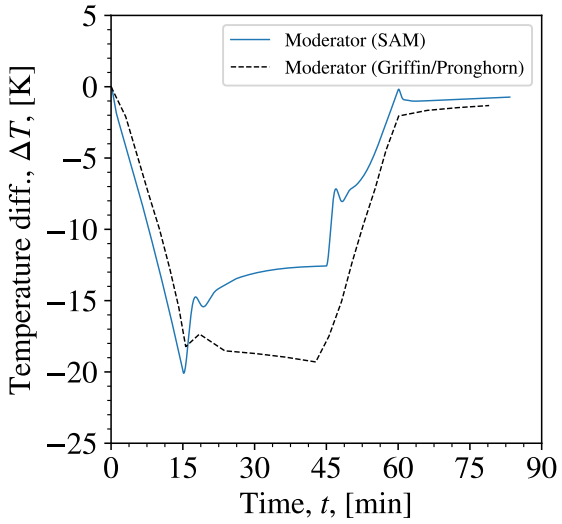

Figure 3.12: Comparison of the moderator temperature change predicted by SAM and Griffin/Pronghorn.

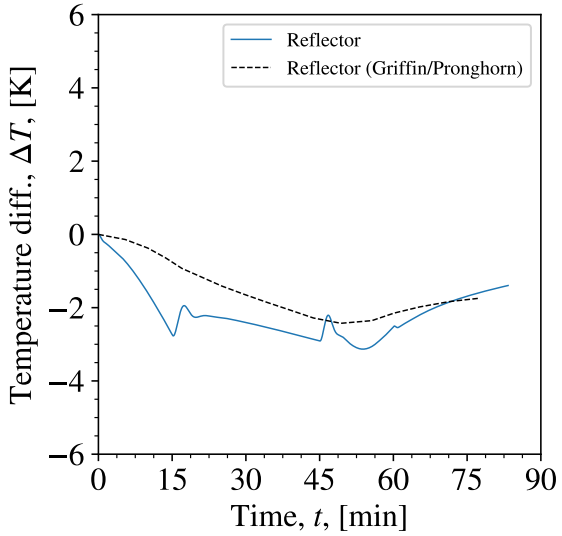

Figure 3.13: Comparison of the reflector temperature change predicted by SAM and Griffin/Pronghorn.

4 Conclusions

This work presents a system-level modeling approach for the core of a generic pebble bed reactor (PBR) using the System Analysis Module (SAM) code. This work is an extension of a previous work by the authors (Ooi et al. (2021)) that used the so-called 2-D ring model approach to model the PBMR-400. With the new approach, the pebble bed of the reactor is modeled with multiple *PBCoreChannel* components with spherical heat structures which

avoids the geometry approximation made in the 2-D ring model, and allows the code to calculate thermal fluid parameters with built-in closure relations. The new core-channel approach is an improvement to the 2-D ring model approach as it does not introduce geometric distortions to the model and thus reduces the uncertainties introduced by necessary geometry approximations.

To verify the model, a simulation under the steady-state normal operating condition is first performed. The results are in a good agreement with the predictions by Stewart et al. (2021) with Griffin/Pronghorn. Furthermore, a load-following transient simulation is carried out to test the fully coupled thermal hydraulics and point kinetics (PKE) aspects of the model. PKE parameters such as the prompt neutron generation time, the delayed neutron precursor fractions, the delayed neutron precursor time constants, and the reactivity feedback coefficients are obtained from the work by Stewart et al. (2021). The prediction by SAM and Griffin/Pronghorn are generally in a good agreement where the overall trends of the predicted reactivities and temperatures are similar. Nevertheless, some discrepancies still remain in terms of the values of these predictions. Given the differences in the approaches between the two codes, with SAM being a system-level code and Pronghorn being a porous-medium code, such discrepancies are expected. Nevertheless, as future steps, continuous efforts will be invested to further improve the current model and the model will be tested with more transient scenarios to ensure its validity and accuracy.

ACKNOWLEDGEMENTS

This work is supported by U.S. DOE Office of Nuclear Energy's Nuclear Energy Advanced Modeling and Simulation (NEAMS) program. The submitted manuscript has been created by UChicago Argonne LLC, Operator of Argonne National Laboratory ("Argonne"). Argonne, a U.S. Department of Energy Office of Science laboratory, is operated under Contract No. DE-AC02-06CH11357. The authors would like to acknowledge the support and assistance from Dr. Ryan Stewart and Dr. Paolo Balestra of Idaho National Laboratory in the completion of this work.

REFERENCES

P. Balestra, S. Schunert, R. W. Carlsen, A. Novak, M. D. DeHart, and D. Martineau. PBMR-400 benchmark solution of exercise 1 and 2 using the MOOSE based applications: MAMMOTH, Pronghorn. volume 247, page 6020. EPJ Web of Conferences, 2021.

H. Gerwin, W. Scherer, A. Lauer, and I. Clifford. TINTE – Nuclear Calculation Theory Description Report. Technical Report ISSN 0944-2952, Institute for Energy Research (IEF): Safety Research and Reactor Technology (IEF-6), 2010.

W. Hahn and E. Achenbach. Determination of the wall heat transfer coefficient in pebble beds. Technical Report Juel-2093, Kernforschungsanlage Juelich G.m.b.H. (Germany, F.R.). Inst. fuer Reaktorbauelemente, 1986.

R. Hu, L. Zou, G. Hu, D. Nunez, T. Mui, and T. Fei. SAM Theory Manual. Technical Report ANL/NSE-17/4 Rev. 1, Argonne National Laboratory, 2021.

E. Merzari, H. Yuan, M. Min, D. Shaver, R. Rahaman, P. Shriwise, P. Romano, A. Talamo, Y.-H. Lan, D. Gaston, et al. Cardinal: A lower-length-scale multiphysics simulator for pebble-bed reactors. *Nuclear Technology*, 207(7):1118–1141, 2021.

NEA. PBMR Coupled Neutronics/ Thermal-hydraulics Transient Benchmark: The PBMR-400 Core Design - Volume 1: The Benchmark Definition. Technical Report NEA/NSC/DOC(2013)10, Organisation for Economic Co-operation and Development-Nuclear Energy Agency, 2013.

A. Novak, R. Carlsen, S. Schunert, P. Balestra, D. Reger, R. Slaybaugh, and R. Martineau. Pronghorn: A multidimensional coarse-mesh application for advanced reactor thermal hydraulics. *Nuclear Technology*, 207(7):1015–1046, 2021.

Z. Ooi, L. Zou, T. Hua, and R. Hu. System-Level Simulation of the PBMR-400 Core with SAM. ANS Winter Meeting and Technology Expo, 2021.

R. Stewart, D. Reger, and P. Balestra. Demonstrate Capability of NEAMS Tools to Generate Reactor Kinetics Parameters for Pebble-Bed HTGRs Transient Modeling. Technical Report INL/EXT-21-64176, Idaho National Laboratory, August 2021.

W. van Antwerpen, C. G. Du Toit, and P. G. Rousseau. A review of correlations to model the packing structure and effective thermal conductivity in packed beds of mono-sized spherical particles. *Nuclear Engineering and Design*, 240(7):1803–1818, 2010.

W. van Antwerpen, R. G. Rousseau, and C. G. du Toit. Multi-sphere Unit Cell model to calculate the effective thermal conductivity in packed pebble beds of mono-sized spheres. *Nuclear Engineering and Design*, 247:183–201, 2012.

L. Zou and R. Hu. Recent SAM Code Improvement to Heat Transfer Modeling Capabilities. Technical Report ANL/NSE-19/46, Argonne National Laboratory, 2019.

Nuclear Science and Engineering Division
Argonne National Laboratory
9700 South Cass Avenue, Bldg. 208
Argonne, IL 60439

www.anl.gov

Argonne National Laboratory is a U.S. Department of Energy laboratory managed by UChicago Argonne, LLC